HSulf-1 and palbociclib exert synergistic antitumor effects on RB-positive triple-negative breast cancer

FENGXIA CHEN[1,2], ZHICAI ZHANG[3], YIHAN YU[4], QIUYU LIU[5] and FEIFEI PU[6]

[1]Department of Medical Oncology, General Hospital of The Yangtze River Shipping, Wuhan Polytechnic University, Wuhan, Hubei 430010; [2]Department of Radiation and Medical Oncology, Zhongnan Hospital of Wuhan University, Wuhan, Hubei 430071; [3]Department of Orthopedics, Union Hospital, Tongji Medical College, Huazhong University of Science and Technology, Wuhan, Hubei 430022; [4]Department of Pediatrics, The Third Xiangya Hospital, Xiangya School of Medicine, Central South University, Changsha, Hunan 410013; [5]Department of Pathology, Henan Provincial People's Hospital, Zhengzhou University, Zhengzhou, Henan 450003; [6]Department of Orthopedics, Union Hospital, Tongji Medical College, Huazhong University of Science and Technology, Wuhan, Hubei 430022, P.R. China

Received January 4, 2020; Accepted April 9, 2020

DOI: 10.3892/ijo.2020.5057

Abstract. Human sulfatase-1 (HSulf-1) is emerging as a novel prognostic biomarker in breast cancer. Previous studies demonstrated HSulf-1 to function as a negative regulator of cyclin D1 in breast cancer. Accumulating preclinical evidence is supporting the efficacy of cyclin-dependent kinase (CDK) 4/6 inhibitors against the luminal androgen receptor sub-type of triple-negative breast cancer (TNBC). It was therefore hypothesized that HSulf-1 may cooperate with CDK4/6 inhibitors to control cell cycle progression in breast cancer cells. HSulf-1 expression was found to be downregulated in TNBC tissues and cell lines compared with that in healthy tissues and non-breast cancer cell lines, respectively. High levels of HSulf-1 expression was also found to be associated with increased progression-free survival and overall survival in patients with TNBC. Functionally, it was demonstrated that HSulf-1 served as tumor suppressor in TNBC by inducing cell cycle arrest and apoptosis whilst inhibiting proliferation, epithelial-mesenchymal transition, migration and invasion. Subsequent overexpression of HSulf-1 coupled with treatment with the CDK4/6 inhibitor palbociclib exhibited a synergistic antitumor effect on retinoblastoma (RB)-positive TNBC. Further studies revealed the mechanism underlying this cooperative antiproliferative effect involved to be due to the prohibitive effects of HSulf-1 on the palbociclib-induced accumulation of cyclin D1 through AKT/STAT3 and ERK1/2/STAT3 signaling. Taken together, findings from the present study not only suggest that HSulf-1 may be a potential therapeutic target for TNBC, but also indicate that combinatorial treatment could be an alternative therapeutic option for RB-positive TNBC, which may open novel perspectives.

Correspondence to: Dr Feifei Pu, Department of Orthopedics, Union Hospital, Tongji Medical College, Huazhong University of Science and Technology, 1277 Jiefang Avenue, Wuhan, Hubei 430022, P.R. China
E-mail: pufeifeiemail@163.com

Key words: retinobalastoma-positive-triple-negative breast cancer, human sulfatase-1, palbociclib, AKT/STAT3, ERK1/2/STAT3

Introduction

Triple-negative breast cancer (TNBC), which accounts for 10-20% of all types of breast cancers (1,2), is characterized by the lack of estrogen receptor (ER) and progesterone receptor expression in addition to the absence of human epidermal growth factor receptor 2 (HER2) amplification. Although it exhibits positive responses to chemotherapy, TNBC remain the most aggressive sub-type among younger patients since it is associated with a worse outcome and a higher risk of relapse within 5 years compared with other sub-types of breast cancer (3-7). Treatment of patients with TNBC has always been challenging due to the absence of effective therapeutic targets. Recently, olaparib, an inhibitor of poly (adenosine diphosphate-ribose) polymerase, has demonstrated promising antitumor activity in HER2-negative patients with a germline mutation in the BRCA gene (8). Although BRCA germline mutations have a relatively higher prevalence in TNBC compared with that in the non-TNBC sub-types, its prevalence in TNBC is only 12% (9,10), severely limiting the efficacy of this treatment strategy. Consequently, there is an urgent need to identify promising alternative treatment strategies for TNBC.

A hallmark of cancer is the dysregulation of cell division, ultimately favoring aberrant proliferation that fuels tumorigenesis and disease progression (11). The cyclin-dependent kinase (CDK)-retinoblastoma (RB)-E2F axis controls transition through the G_1/S cell cycle checkpoint. CDK4/6 first forms a complex with cyclin D1 to promote the phosphorylation of the RB protein (12). Phosphorylated (p)-RB then allows the dissociation of transcription factor E2F from the pRb–E2F complex to promote G_1/S transition (12). Inhibition of CDK4/6 results in

RB dephosphorylation, leading to cell cycle arrest (12). Since CDK4/6 activity is frequently dysregulated and constitutively active in breast cancer cells, inhibition of CDK4/6 may prove to be an effective therapeutic intervention against breast cancer (2). Treatment using highly selective CDK4/6 inhibitors, including palbociclib, ribociclib and abemaciclib, have been previously reported to improve progression-free survival (PFS) in the first and later lines of ER^+ metastatic breast cancer therapy (13-18). Since TNBC is a group of highly proliferative tumors enriched in cell cycle genes, intrinsic resistance to CDK4/6 inhibitor monotherapy has been observed owing to the loss or mutation of RB (19-21). By contrast, it was also reported that the loss of RB in TNBC can result in improved response to chemotherapy (22-24). The Cancer Genome Atlas study revealed that since only 20% of patients with TNBC carry mutations in RB or are RB-negative, the use of CDK4/6 inhibitors may serve as a promising therapeutic strategy for RB-positive TNBC (2).

Human sulfatase-1 (HSulf-1) is an endosulfatase that selectively removes 6-O-sulfate from heparan sulfate proteoglycans (HSPGs) in the extracellular matrix (25). The sulfation of HSPG residues is required for their interaction with a number of heparin-binding growth factors (HBGFs), including fibroblast growth factor 2 (FGF-2), hepatocyte growth factor (HGF) and heparin-binding epidermal growth factor (HB-EGF), to promote their activation (25,26). In normal human tissues, HSulf-1 is stably expressed and serves important roles in cell proliferation and differentiation (27). However, HSulf-1 expression has been reported to be downregulated in various tumors, including ovarian, breast and gastric carcinomas (28,29). A number of studies previously revealed that the downregulation of HSulf-1 in cancers is mediated by epigenetic modification, including CpG island methylation and histone acetylation (28,29) Reduced expression of HSulf-1 is one of the causes behind the increased sulfation of HSPGs, leading to excessive activation of the signal transduction pathways downstream of growth factor receptors. Ultimately, this results in cancer cell proliferation, increased metastatic activity, inhibition of apoptosis and reduced sensitivity to radio- and chemotherapy (30-37). Previously, several studies revealed that the overexpression of HSulf-1 inhibited tumor proliferation and angiogenesis in xenografts derived from breast cancer cell lines (36). Additionally, high levels of HSulf-1 have also been found to correlate with increased PFS and overall survival (OS) in patients with breast cancer (38,39). Mechanistically, it was reported that HSulf-1 inhibited autocrine cyclin D1 expression, leading to decreased S phase fractions whilst increasing G_2-M fractions and increased cell death (39). However, the potential relationship between HSulf-1 and CDK4/6 inhibition remains unexplored, which serves as the subject of the present study.

In the present study, HSulf-1 expression level was first measured in TNBC tissues and cell lines, following which the function of HSulf-1 in TNBC was next demonstrated. Secondly, the effects of HSulf-1 overexpression in combination with treatment with the CDK4/6 inhibitor palbociclib on RB-positive TNBC was investigated. Finally, further studies were performed to explore the mechanism underlying this effect. Based on the present study, it could be speculated that HSulf-1 may not only serve as a potential therapeutic target but also a reliable efficacy predictor for CDK4/6 inhibitors. Therefore, in clinical practice, patients with TNBC and elevated HSulf-1 expression can potentially be selected for palbociclib treatment, which may achieve superior therapeutic efficacy.

Materials and methods

Human tissue specimens. In total, 86 tissue TNBC specimens and paired adjacent normal breast tissues were collected from patients with TNBC (sex, all female; age range, 25-73 years; median age, 47) at the General Hospital of The Yangtze River Shipping (Wuhan, China), Wuhan Polytechnic University (Wuhan, China) and the Henan Provincial People's Hospital, Zhengzhou University (Zhengzhou, China) between January 2000 and January 2019. All specimens were collected by surgical resection and the distance between the tumour and adjacent normal tissue was >1 cm. Non-TNBC patients, patients receiving chemotherapy or radiotherapy prior to surgical treatment and pregnancy concomitant with the diagnosis were excluded from the present study. The follow-up time range was 6-210 months. Informed consent was obtained from all patients. This experiment was approved by the Ethics Committee of the General Hospital of The Yangtze River Shipping, Wuhan Polytechnic University (approval no. 2017IEC0003). All specimens were classified according to the 2003 World Health Organization Consensus Classification and the Eighth Edition AJCC Cancer Staging for breast cancer (40,41). Detailed clinicopathological features are shown in Table I.

Immunohistochemistry. Tissue samples were first fixed in 4% formalin for 24 h at room temperature and then embedded in paraffin blocks. Tissue sections (thickness, 4 μm) were subsequently deparaffinized in a graded series of xylene followed by rehydration in a descending series of ethanol before antigen retrieval in citrate buffer (pH 9.0) at 100˚C for 2 min. Then, the tissue sections were blocked for 30 min with 3% BSA (Sigma-Aldrich; Merck KGaA) at room temperature. After incubation with primary anti-HSulf-1 (1:250; cat. no. ab32763; Abcam) at 4˚C overnight and secondary antibodies (biotin-conjugated goat anti-rabbit IgG, 1:400 dilution, cat. no. SA00004-2; Proteintech Group, Inc.) at room temperature for 30 min, the sections were then incubated with avidin-biotin complex-horseradish peroxidase (HRP; Vectastain® ABC kit, Maravai LifeSciences) at 37˚C for 20 min followed by incubation with 3'3-diaminobenzidine (Sigma-Aldrich; Merck KGaA) and counterstained with hematoxylin (Sigma-Aldrich; Merck KGaA) for 5 min at room temperature. The percentage of positively stained cells was scored on a scale of 0 to 4 as follows: i) 0, ≤5%; ii) 1, 6-25%); iii) 2, 26-50%); iv) 3, 50-75%; and v) 4, 76-100%. The staining intensity was scored from 0 to 3 as follows: i) 0, negative); ii) 1, weak; iii) 2, moderate; and iv) 3, strong). The scores for the percentages of positive cells and staining intensities were then multiplied to generate an immunoreactivity score (IS) for each case. The IS ranged from 0-12 (0, 1, 2, 3, 4, 6, 8, 9 and 12). Cut-off values for this scoring system were assigned as follows: i) High HSulf-1 expression, IS ≥4 (4, 6, 8, 9 and 12); ii) low HSulf-1 expression, IS <4 (0, 1, 2 and 3). Tissue slides were visualized under a light microscope (magnification, x400; Olympus FSX100; Olympus Corporation). Five

Table I. Association between HSulf-1 expression and clinicopathologic characteristics of 86 TNBC patients.

Parameters	HSulf-1 expression				P-value[a]
	Low (n=55)	%	High (n=31)	%	
Age (years)					0.4238
≤50	35	67	17	33	
>50	20	59	14	41	
Grade					0.6237
Low	10	59	7	41	
High	45	65	24	35	
Tumor size (cm)					0.5089
≤5	41	63	24	37	
>5	14	67	7	33	
Lymph node metastasis					0.7535
Negative	30	64	17	36	
Positive	25	64	14	36	

[a]χ^2 test. HSulf-1, human sulfatase.

high-power fields were examined randomly for each section. Quantifications of the proteins of interest were performed using the Image Pro Plus 6.0 software (Media Cybernetics, Inc.).

Cell lines and culture. The breast cancer cell lines (Hs578T and MDA-MB-231) human immortalized breast epithelial cell line (MCF10A) and 293T cells were purchased from American Type Culture Collection (ATCC). Hs578T MDA-MB-231 and 293T cells were cultured in DMEM (Gibco; Thermo Fisher Scientific, Inc.) with 10% FBS (Gibco; Thermo Fisher Scientific, Inc.) in a humidified atmosphere at 37˚C in 5% CO^2. MCF10A cells were cultured in DMEM/F12 (Procell Life Science & Technology Co., Ltd.) containing 5% horse serum, 20 ng/ml EGF, 0.5 μg/ml hydrocortisone, 10 μg/ml insulin and 1% NEAA (Procell Life Science & Technology Co., Ltd.) in a humidified atmosphere at 37˚C in 5% CO^2. Palbociclib (Sigma-Aldrich; Merck KGaA) was dissolved in DMSO, following which the cells were treated with 500 nM palbociclib for 72 h at 37˚C. Palbociclib (500 nM) was used for the majority of the experiments as previously described (42,43). An equivalent concentration of DMSO was used as negative control treatment in parallel with palbociclib treatment.

Plasmids, lentivirus production and cell transfection. The plasmids (pcDNA3.0-vector, pcDNA3.0-HSulf-1, pcDNA3.0-cyclin D1, LV105-HSulf-1 and LV105-EGFP) and the vector psi-H1 used for cloning the HSulf-1 short hairpin RNA (shRNA) were purchased from iGene Biotechnology Co., Ltd. Hs578T and MDA-MB-231 cells ($5x10^5$ cells/well) were plated into six-well plates 24 h prior to transfection. Plasmids (2.5 μg/well) were transfected into cells using Lipofectamine® 3000 (Invitrogen; Thermo Fisher Scientific, Inc.) according to the manufacturer's protocol for *in vitro* assays. Cells were incubated for 48 h at 37˚C prior to further experimentation. The lentivirus particles were produced by transfecting 293T cells (ATCC) with pEZ-Lv105 lentiviral vectors encoding HSulf-1 (LV105-HSulf-1) and the control empty vector (LV105-EGFP) using the LentiPac™ Expression packaging kit (GeneCopoeia, Inc.) according to the manufacturer's protocols. The lentivirus-containing supernatants were harvested 72 h following transfection and were filtered through 0.45-μm PVDF filters (EMD Millipore). The supernatant was then concentrated by ultracentrifugation at 100,000 x g for 2 h at room temperature. MDA-MB-231 cells ($4x10^5$ cells/well; multiplicity of infection, 10) were infected with the lentiviral particles ($2.03x10^8$ TU/ml) where the stable cell lines were established by treatment with puromycin (2.5 μg/ml) for 2 weeks at 37˚C for *in vivo* study. Transfection efficiency was determined by reverse transcription-quantitative PCR (RT-qPCR) and western blot analysis. The target sequences used for shRNA were as follows: ShHSulf-1 1, 5'-CCCAAA TATGAACGGGTCAAA-3' and shHSulf-1 2, 5'-CCAAGA CCTAAGAATCTTGAT-3'. The plasmid shHSulf-11 was chosen for further study based on its superior silencing effect.

RT-qPCR. Total RNA was extracted from MDA-MB-231 cells transfected with the HSulf-1 overexpression or vector plasmid using RN07-EASYspin kit (Aidlab Biotechnologies Co., Ltd) according to manufacturer's protocols. cDNA was then synthesized using the PrimeScript™ RT Master Mix (Takara Bio, Inc.) from 1 μg RNA according to manufacturer's protocols The following temperature protocol was used for the reverse transcription reaction: 37˚C for 15 min, followed by reverse transcriptase inactivation reaction: 85˚C for 5 sec. qPCR reactions were performed using SYBR® Premix Ex Taq™ (Takara Bio, Inc.) according to manufacturer's protocols. The thermocycling conditions were as follows: Initial denaturation at 95˚C for 30 sec, followed by 40 cycles of 95˚C for 5 sec and 60˚C for 30 sec. Relative expression was calculated using the $2^{-\Delta\Delta Cq}$ method (44). GAPDH was used as an internal control. The sequences of the primers were as follows: Cyclin D1 forward,

5'-CCCACTCCTACGATACGC-3' and reverse, 5'-AGCCTC CCAAACACCC-3'; GAPDH forward, 5'-GGAGCGAGATCC CTCCAAAAT-3' and reverse, 5'-GGCTGTTGTCATACT TCTCATGG-3'.

Western blotting. Protein extracts were prepared using RIPA buffer (Thermo Fisher Scientific, Inc.) supplemented with protease and phosphatase inhibitors. Protein concentrations were determined using a bicinchoninic acid protein assay kit (Thermo Fisher Scientific, Inc.). A total of 20 μg total protein was loaded per lane and separated by SDS-PAGE (10 or 12% gels) before transferal to polyvinylidene fluoride membranes (EMD Millipore). The membranes were blocked in 5% skimmed milk diluted with Tris-buffered saline/Tween-20 (0.1%) (TBS-T) at room temperature for 1 h and subsequently incubated overnight at 4˚C with the following primary antibodies: Anti-RB (1:1,000, cat. no. 9309; Cell Signaling Technology, Inc.), anti-p-RB (1:1,000, Ser780; cat. no. 9307; Cell Signaling Technology, Inc.), anti-HSulf-1 (1:1,000, cat. no. ab32763; Abcam), anti-E-cadherin (1:500, cat. no. ab15148; Abcam), anti-vimentin (1:1,000, cat. no. ab92547; Abcam), anti-N-cadherin (1:2,000, cat. no. ab76011; Abcam), anti-cyclin D1 (1:200, cat. no. ab16663; Abcam), anti-STAT3 (1:1,000, cat. no. 30835; Cell Signaling Technology, Inc.), anti-p-STAT3 (Y705; 1:2,000, cat. no. 9145; Cell Signaling Technology, Inc.), anti-JAK2 (1:1,000, cat. no. 74987; Cell Signaling Technology, Inc.), anti-p-JAK2 (Tyr1007; 1:1,000, cat. no. 4406; Cell Signaling Technology, Inc.), anti-AKT (1:1,000, cat. no. 9272; Cell Signaling Technology, Inc.), anti-p-AKT (Ser473; 1:1,000, cat. no. 9271; Cell Signaling Technology, Inc.), anti-ERK1/2 (1:1,000, cat. no. 4695; Cell Signaling Technology, Inc.), anti-pERK1/2 (Thr202/Tyr204; 1:2,000, cat. no. 4370; Cell Signaling Technology, Inc.), anti-GAPDH (1:5,000, cat. no. 60004-1-Ig; Proteintech Group, Inc.), and anti-β-actin (cat. no. 60008-1-Ig; Proteintech Group, Inc.). The next day, the membranes were washed with TBS-T and then incubated with secondary antibodies including horseradish peroxidase-conjugated goat anti-mouse (1:10,000, cat. no. SA00001-1; Proteintech Group, Inc.) and goat anti-rabbit (1:10,000, cat. no. SA00001-2; Proteintech Group, Inc.) at 37˚C for 1 h. Immunoreactive bands were visualized using ECL reagent (Advansta, Inc.) and detected using the ChemiDoc XRS+ system (Bio-Rad Laboratories, Inc.). Gray values were calculated using ImageJ software (version 1.52u; National Institutes of Health).

Cell counting kit-8 (CCK-8) assay. Hs578T and MDA-MB-231 cells (3,000 cells/well) were first seeded into 96-well plates in triplicate, allowed to attach for 24 h at 37˚C and treated with the indicated concentrations of palbociclib for 0, 24, 48 and 72 h at 37˚C. Subsequently, 10 μl CCK-8 solution (MedChemExpress) was added into each well before the plates were subsequently incubated for 4 h at 37˚C. The optical density was measured at 450 nm using the SpectraMax M5 microplate reader (Molecular Devices, LLC).

Colony formation assay. Cells were seeded in 6-well plates at a density of 1,000 cells per well. After 24 h of culture at 37˚C, the Hs578T and MDA-MB-231 cells were transfected with the HSulf-1 overexpression or vector plasmid and then treated with 500 nM palbociclib for 14 days at 37˚C. After 14 days, cell colonies were fixed with 4% paraformaldehyde and stained with 0.1% crystal violet, each for 30 min at room temperature. Cell colonies containing >50 cells were counted using the ImageJ software (version 1.52u; National Institutes of Health) and images were taken with a camera (Canon, Inc.).

Cell cycle assay. Hs578T and MDA-MB-231 cells were harvested and fixed with 70% cold ethanol at 4˚C overnight, following which the cells ($8x10^5$/tube) were washed with PBS twice, mixed with 400 μl propidium iodide (PI) (Beyotime Institute of Biotechnology) and incubated for 30 min in the dark at room temperature and then analyzed by flow cytometry (Cytoflex, Beckman Coulter, Inc.) with a CytExpert software (version 2.3; Beckman Coulter, Inc.). Each sample was tested in triplicate.

Apoptosis analysis. Hs578T and MDA-MB-231 cell apoptosis was analyzed by flow cytometry (CytoFLEX; Beckman Coulter, Inc.) as per the FITC-conjugated Annexin V/PI method (Annexin V-FITC/PI Apoptosis Kit; Beyotime Institute of Biotechnology). After 72 h of the indicated treatment, adherent and suspended cells ($3x10^5$/tube) were both harvested by centrifugation and resuspended in 195 μl binding buffer, following which Annexin V-FITC (5 μl) and PI (10 μl) were added to each sample and mixed. Cells were incubated for 15 min in the dark at 4˚C and then analyzed by flow cytometry (Cytoflex; Beckman Coulter, Inc.) using a CytExpert software (version 2.3; Beckman Coulter, Inc.). Each sample was tested in triplicate.

Wound-healing assay. Hs578T and MDA-MB-231 cells were seeded into six-well plates at a density of $5x10^5$ cells per well and allowed to attach for 24 h at 37˚C. Plasmids (pcDNA3.0-vector, pcDNA3.0-HSulf-1, shNC and shHSulf-1) were transfected into cells and then treated with 500 nM palbociclib for 72 h 37˚C. Cells were harvested and reseeded into six-well plates ($1x10^6$ cells/well) and cultured to 90% confluence. A 200 μl sterile pipette tip was then used to scratch a wound (time 0 h), following which fresh low-serum (2% FBS) DMEM was immediately replaced after three times of washing with PBS. Cell migration was imaged under a light microscope (magnification, x100; Olympus Corporation) at 0 and 24 h after the injury. The wound width was evaluated by measuring the distance between the two edges of the scratch at five sites in each image. Cell migration was determined using the following formula: Percentage of wound healing (%) = [(wound width at the 0 h time point-wound width at the 24 h time point)/wound width at the 0 h time point] x100.

Transwell assay. Transwell chambers (Corning, Inc.) were coated with 50 μl of DMEM-diluted Matrigel (1:8 dilution; BD Biosciences) which was precooled at 4˚C for 12 h and then incubated overnight at 37˚C. Cells were suspended in serum-free culture medium ($5x10^4$ cells/well). A total of 200 μl cell suspension was transferred into the upper chambers whilst 600 μl DMEM supplemented with 10% FBS was added to the lower chambers. After 24 h incubation, the cells that migrated to the lower chambers were fixed with 4% paraformaldehyde and stained with 0.1% crystal violet each for 30 min at room

temperature. The number of migratory cells were counted from three randomly chosen fields per chamber under a light microscope (magnification, x100; Olympus Corporation).

Tumor xenografts. Animal experiments were performed with the approval of the Animal Care and Use Committee of the General Hospital of The Yangtze River Shipping, Wuhan Polytechnic University (approval no. 2017IEC0003; Wuhan, China). A total of 12 four-week-old female BALB/c nude mice were maintained under standard conditions (room temperature, 22±2˚C; relative humidity, 55±10%) on a 12-h light/dark cycle (lights on at 6:00 a.m.), where they had *ad libitum* access to food and water. A daily observation was preformed to prevent the animals from anger, restlessness, fear, anxiety, pain or damage to keep them at a normal status. These mice (age, 4 weeks) were randomly divided into two groups (n=6 mice/group). MDA-MB-231 cells ($2x10^7$) stably transfected with LV105-HSulf-1 plasmids or the control vector were suspended in 100 ml PBS and subcutaneously injected into the nude mice under the axilla of the left forelimb. Once the tumors of the control vector group reached ~300 mm^3, mice with tumors of similar size were distributed into the treatment cohorts (n=3/group). Mice were orally treated with 50 mg/kg palbociclib dissolved in 0.5% methylcellulose or vehicle (0.5% methylcellulose) daily for 21 days. Tumor sizes were monitored every 3 days for 3 weeks. At the completion of 3 weeks of palbociclib treatment, all 12 mice were euthanized by cervical dislocation. Death was confirmed by the cessation of breathing, muscle relaxation and the absence of nerve reflex. The experiment lasted a total of 6 weeks. No accidental death was observed before these mice were euthanized. The tumors were then excised and measured. The length (l) and width (w) of each tumor were measured using digital calipers, where tumor volumes were calculated according to the following formula: Tumor volume (V)=$lxw^2x0.5$.

Statistical analysis. Statistical analyses were performed using GraphPad Prism 8.0 software (Graphpad Software, Inc.). Data are presented as the means ± standard deviation. Data were analyzed using Student's t-test or one-way ANOVA followed by either Dunnett's or Tukey's post hoc test. Wilcoxon-signed rank sum test and the χ^2 test was used to analyze the IHC data, whilst the log-rank test was used to assess the statistical significance of the Kaplan-Meier plots and Cox proportional-hazards model was used to determine the hazard ratio and 95% CI. $P<0.05$ were considered to indicate a statistically significant difference.

Results

HSulf-1 is downregulated in TNBC tissues and cell lines and high HSulf-1 levels associate with improved prognosis in patients with TNBC. It was demonstrated previously that HSulf-1 expression was downregulated in ~60% of breast cancers, which was in turn associated with poor patient prognosis (38,39). Therefore, the expression levels of HSulf-1 in 86 pairs of TNBC and adjacent normal mammary tissues were first measured, where it was found that HSulf-1 expression was significantly downregulated in TNBC tissues compared with that in the paired normal tissues (Fig. 1A and B). In addition, higher expression levels of HSulf-1 was found to significantly associate with prolonged PFS (HR, 1.943; 95% CI, 1.054–3.581; P=0.025) and OS (HR, 2.159; 95% CI, 1.041–4.478; P=0.032) in TNBC (Fig. 1C and D). However, HSulf-1 levels showed no significant associations with the clinicopathological indicators, including age, tumor grade, tumor size and lymph node status (Table I). A number of preclinical studies previously suggested that CDK4/6 inhibitors exerted inhibitory effects in RB-positive TNBC cell lines (43,45-47). Therefore, two RB-positive cell lines Hs578T and MDA-MB-231 were chosen to examine the expression levels of HSulf-1 and RB phosphorylation in these two cell lines and one human immortalized breast epithelial cell line MCF10A (43,47). HSulf-1 expression also was also found to be significantly downregulated in Hs578T and MDA-MB-231 compared with that in MCF10A (Fig. 1E). Collectively, these data suggested that HSulf-1 expression was downregulated in TNBC tissues and cells, where reduced HSulf-1 expression was highly predictive of poor patient prognosis.

Overexpression of HSulf-1 inhibits cell proliferation and exhibits a synergistic antiproliferative effect with palbociclib on RB-positive TNBC cells, both in vitro and in vivo. To explore the effects of HSulf-1 and/or palbociclib treatment on TNBC cell proliferation, an HSulf-1 overexpression plasmid was transfected into Hs578T and MDA-MB-231 cells. CCK-8 assay was performed to measure cell viability following treatment with palbociclib for various periods of time (0, 24, 48 and 72 h). Overexpression of HSulf-1 was found to significantly reduce the viability of TNBC cells compared with those transfected with the control vector (Fig. 2A). In addition, combined HSulf-1 overexpression and palbociclib treatment synergistically potentiated the reduction of cell viability compared with that following either intervention alone (Fig. 2A). Colony formation assays yielded similar trends of results (Fig. 2B). By contrast, downregulation of HSulf-1 expression using shRNAs was found to significantly increase proliferation compared with cells transfected with the control vector (Fig. S1A-C).

The effects of HSulf-1 overexpression and/or palbociclib treatment on tumor proliferation was next investigated *in vivo*. MDA-MB-231 cells stably expressing either the control vector or HSulf-1 overexpression plasmid were injected into female nude mice to form xenografts. The xenograft models were treated with 50 mg/kg palbociclib dissolved in 0.5% methylcellulose or vehicle daily for 21 consecutive days. Treatment with palbociclib or overexpression of HSulf-1 alone was found to significantly hinder tumor growth compared with tumors in the Lv105-EGFP + vehicle group. (Fig. 2C). Combined treatment with palbociclib and HSulf-1 overexpression potentiated the reduction in tumor volume compared with that following either interventions alone (Fig. 2C). Collectively, these results suggested that the combination of HSulf-1 overexpression and palbociclib treatment co-operatively inhibited the proliferation of RB-positive TNBC cells both *in vitro* and *in vivo*.

HSulf-1 and palbociclib exhibit a cooperative antitumor effect by inducing G_1/S cell cycle arrest, inhibiting migration, invasion and epithelial-to-mesenchymal transition (EMT) in RB-positive TNBC in vitro. To investigate the biological

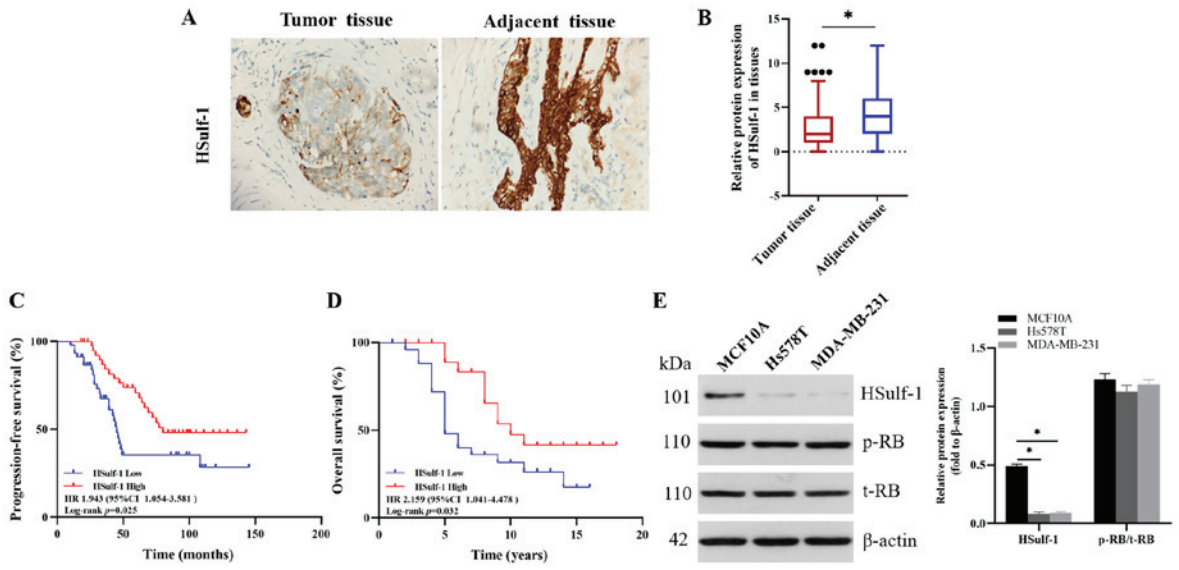

Figure 1. Detection of HSulf-1 expression in TNBC and its association with patient survival. (A) Representative immunohistochemistry images for HSulf-1 staining in paraffin-embedded tumor and adjacent normal mammary tissues from 86 patients with TNBC. (B) The relative protein expression of HSulf-1 was detected using immunohistochemistry in 86 pairs of TNBC tissues and paired adjacent normal breast tissues (C) Association between HSulf-1 expression levels and progression-free survival in the 86 patients with TNBC. (D) Association between HSulf-1 expression levels and overall survival in 86 patients with TNBC. (E) HSulf-1 expression, RB phosphorylation and total RB expression were measured by western blotting in Hs578T, MDA-MB-231 and MCF10A cells. β-actin was used as an internal control. The results were derived from three independent experiments. Data are presented as the mean ± SD. *P<0.05. TNBC, triple-negative breast cancer; HSulf-1, human sulfatase-1; RB, retinoblastoma; p-, phosphorylated; t-, total; HR, hazard ratio; CI, confidence interval.

effects of HSulf-1 and palbociclib in RB-positive TNBC cells further, the following experiments were performed. Cell cycle analysis indicated that palbociclib treatment significantly inhibited S phase entry, whilst HSulf-1 overexpression increased the % of cells in the G_1 and G_2 phases of the cell cycle (Fig. 3A). The combination of HSulf-1 overexpression and palbociclib treatment enhanced G_1 arrest in RB-positive TNBC cells further compared with either treatments alone (Fig. 3A). Apoptosis analysis revealed that palbociclib treatment had no impact on the apoptosis of TNBC cells (Fig. 3B). By contrast, significantly increased apoptosis was observed in the HSulf-1-overexpressing TNBC cells compared with those transfected with the control vector (Fig. 3B). These results suggested that the cooperative antiproliferative effect of the combinatorial treatment was dependent on the induction of G_1/S cell cycle arrest instead of the apoptosis of RB-positive TNBC cells.

The anti-metastatic effect of palbociclib on TNBC remains controversial (48-51). As a result of these contradictory reports, the potential anti-migratory and anti-invasive properties of palbociclib in the two RB-positive TNBC cell lines were investigated. Overexpression of HSulf-1 or palbociclib treatment alone significantly impaired the migration and invasion of Hs578T and MDA-MB-231 cells compared with those treated with vehicle and transfected with the control vector (Fig. 3C and D). By contrast, when HSulf-1 expression was downregulated using shRNAs, it was shown that the migratory and invasive abilities of Hs578T and MDA-MB-231 cells were significantly increased compared with those transfected with the control vector (Fig. S1D and E). Additionally, palbociclib treatment combined with HSulf-1 overexpression significantly enhanced the anti-migratory and invasive effects further compared with those following either treatment alone (Fig. 3C and D). Since EMT is typically the first crucial process in cancer metastasis (52-55), potential changes in the expression of EMT markers was examined. Hs578T and MDA-MB-231 cells treated with palbociclib or transfected with the HSulf-1 overexpression plasmid showed significantly increased expression levels of E-cadherin, along with significant reductions in those of vimentin and N-cadherin compared with cells in the control vector+vehicle group (Fig. 3E). When the two interventions were combined, a significant synergistic effect was observed (Fig. 3E). Collectively, these data demonstrated the cooperative antitumor effects of combining palbociclib with HSulf-1 overexpression was mediated via the induction of G_1/S cell cycle arrest and the inhibition of migration, invasion and EMT *in vitro*.

HSulf-1 inhibits cell cycle progression by suppressing the expression of cyclin D1 via non-canonical AKT/STAT3 and ERK1/2/STAT3 signaling. Previous studies reported that HSulf-1 downregulated cyclin D1 expression by inhibiting the STAT3 signaling pathway in hepatocellular carcinoma cells (56). In addition, it was reported that constitutive STAT3 activation occurs in >40% of breast cancers, especially in the triple-negative sub-type (31,57). Therefore, to ascertain if HSulf-1 regulated cyclin D1 expression in TNBC cells via the STAT3 pathway, HSulf-1 was overexpressed in TNBC cells, following which the expression levels of the associated critical signaling components were evaluated *in vitro*. Overexpression of HSulf-1 significantly reduced cyclin D1 expression and STAT3 phosphorylation without affecting total STAT3 expression in TNBC cells compared with those transfected with the control vector (Fig. 4A). Additionally, it was hypothesized that HSulf-1 could inhibit the expression of cyclin D1 through the canonical JAK2/STAT3 pathway. Subsequent measurement of

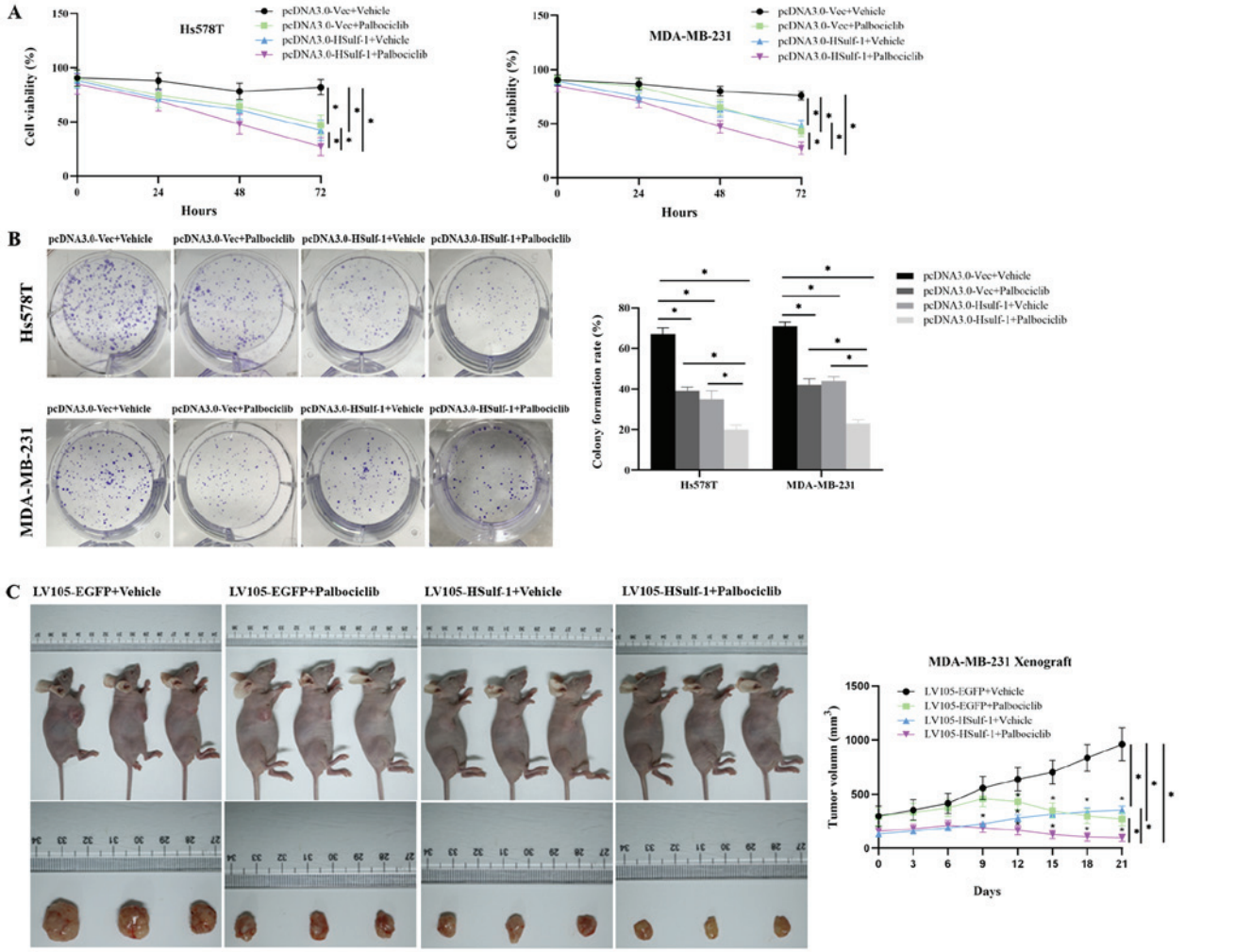

Figure 2. HSulf-1 inhibits cell proliferation and when combined with palbociclib, exerts antiproliferative effects on RB-positive TNBC cells in a synergistic manner both *in vitro* and *in vivo*. (A) Hs578T and MDA-MB-231 cells were transiently transfected with the control vector or HSulf-1 overexpression plasmids and incubated for 6 h at 37˚C then incubated with fresh complete medium cantaining 500 nM palbociclib or DMSO for 0, 24, 48 and 72 h. Subsequently, Cell Counting Kit-8 assays were performed to assess cell viability. (B) Hs578T and MDA-MB-231 cells were transiently transfected with the control vector or HSulf-1 overexpression plasmids and incubated for 6 h at 37˚C then incubated with fresh complete medium containing 500 nM palbociclib or DMSO for up to 14 days for colony formation assay. (C) Representative images of the mouse xenograft models and tumors extracted from the four treatment groups after euthanasia. The results were derived from three independent experiments. Data are presented as the mean ± SD. *P<0.05. TNBC, triple-negative breast cancer; HSulf-1, human sulfatase-1; RB, retinoblastoma; EGFP, enhanced green fluorescent protein.

JAK2 phosphorylation and total JAK2 expression in parental and HSulf-1-overexpressing cells showed that neither were significantly unaffected by HSulf-1 overexpression (Fig. 4B).

Previous studies have also reported that HSulf-1 inhibited the AKT and ERK signaling pathways, leading to cell cycle arrest, apoptosis, suppression of EMT and suppression of metastasis (34,39,58-61). Additionally, it has been demonstrated that ERK1/2 can directly phosphorylate Ser727 at the C-terminus of STAT3 (62). Malanga *et al* previously showed that suppression of AKT reduces the phosphorylation and transcriptional activity of STAT3, whereas the opposite effects were observed following AKT activation in non-small cell lung cancer cells (63). Based on these previous observations, it was hypothesized that HSulf-1 may suppress STAT3 activity via the ERK1/2 and AKT signaling pathways. Overexpression of HSulf-1 was found to significantly attenuate ERK1/2, AKT and STAT3 phosphorylation in MDB-MB-231 cells compared with those transfected with the control vector (Fig. 4C). In conclusion, these observations suggest that HSulf-1 suppressed cyclin D1 expression via non-canonical AKT/STAT3 and ERK1/2/STAT3 signaling but not the canonical JAK2/STAT3 pathway, leading to cell cycle arrest and the inhibition of proliferation of TNBC cells both *in vitro* and *in vivo*.

HSulf-1 cooperates with palbociclib to induce antiproliferative effects by reducing palbociclib-induced cyclin D1 accumulation. A recently published preclinical study reported that a novel CDK4/6 inhibitor, SHR6390, increased the expression of cyclin D1 in RB-positive MCF7 cells without affecting the RB-negative TNBC cell line MDA-MB-468 (64). To determine if palbociclib can exert a similar effect on RB-positive TNBC cells, cyclin D1 expression was next measured following palbociclib treatment. It was found that following palbociclib treatment, the levels of RB expression and phosphorylation were significantly reduced, whilst that of cyclin D1 expression was significantly increased compared with those treated with vehicle (Fig. 5A). In addition, palbociclib-induced cyclin D1 accumulation was found to be significantly reduced following the overexpression of HSulf-1,

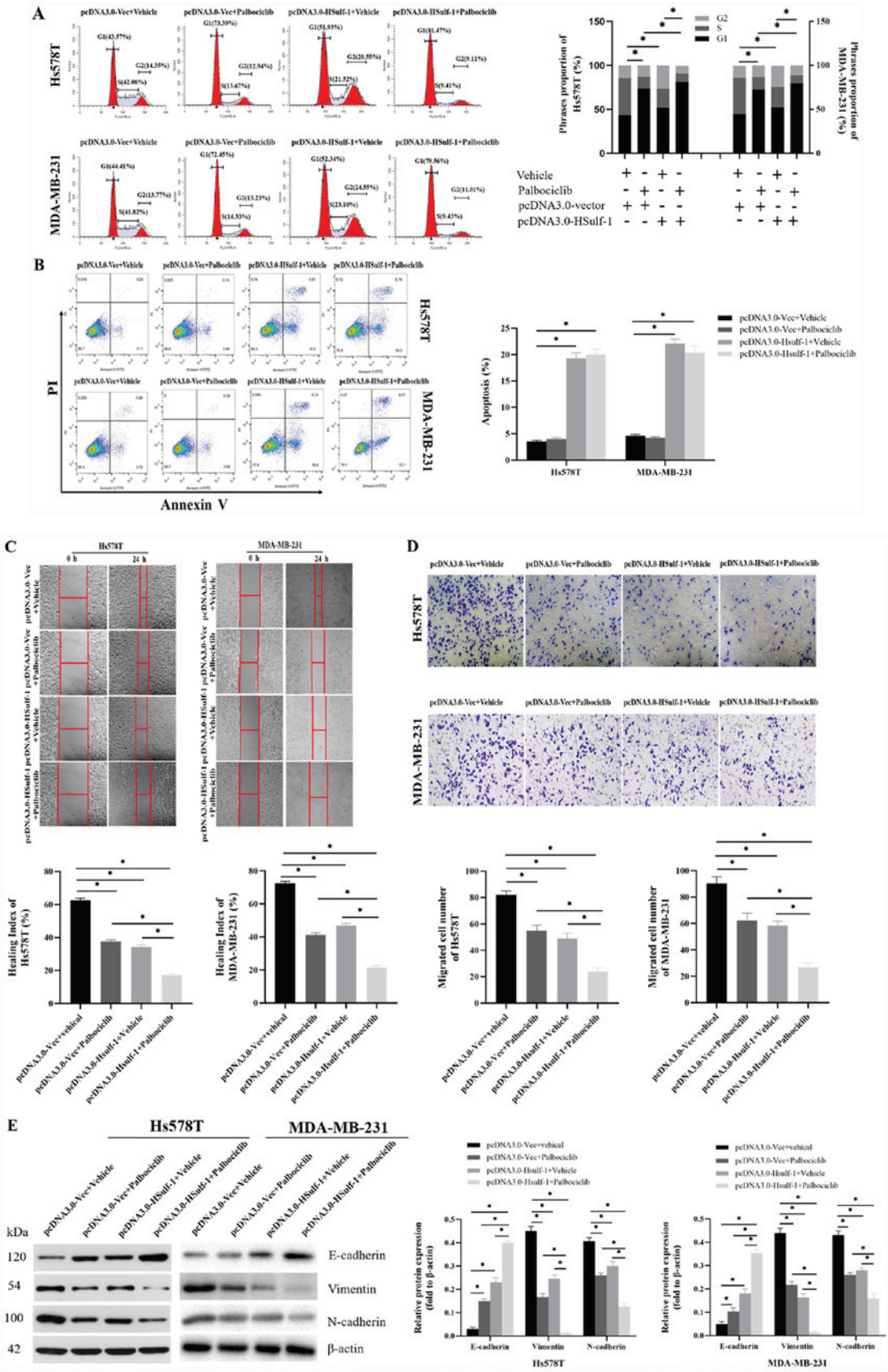

Figure 3. HSulf-1 in combination with palbociclib exerts synergistic antitumor effects by inducing G_1/S stage cell cycle arrest and by inhibiting migration, invasion and epithelial-mesenchymal transition *in vitro*. (A-E) Hs578T and MDA-MB-231 cells following transient transfection with the control vector or HSulf-1 overexpression plasmids and incubation with 500 nM palbociclib or DMSO for 72 h. (A) Cell cycle analysis. G_1 and S phases of pcDNA3.0-Vector+Vehicle vs. pcDNA3.0-Vector+Palbociclib; G_1 and G_2 phases of pcDNA3.0-Vector+Vehicle vs. pcDNA3.0-HSulf-1+Vehicle; G_1 phase of pcDNA3.0-Vector+Palbociclib vs. pcDNA3.0-HSulf-1+Palbociclib; G_1 phase of pcDNA3.0-HSulf-1+Vehicle vs. pcDNA3.0-HSulf-1+Palbociclib. (B) Apoptosis analysis. (C) Wound healing assays. (D) Transwell assays. Magnification, x100. (E) Western blotting was performed to measure E-cadherin, vimentin and N-cadherin expression, with β-actin used as an internal control. The results were derived from three independent experiments. Data are presented as the mean ± SD. *P<0.05. HSulf-1, human sulfatase-1; vec, vector.

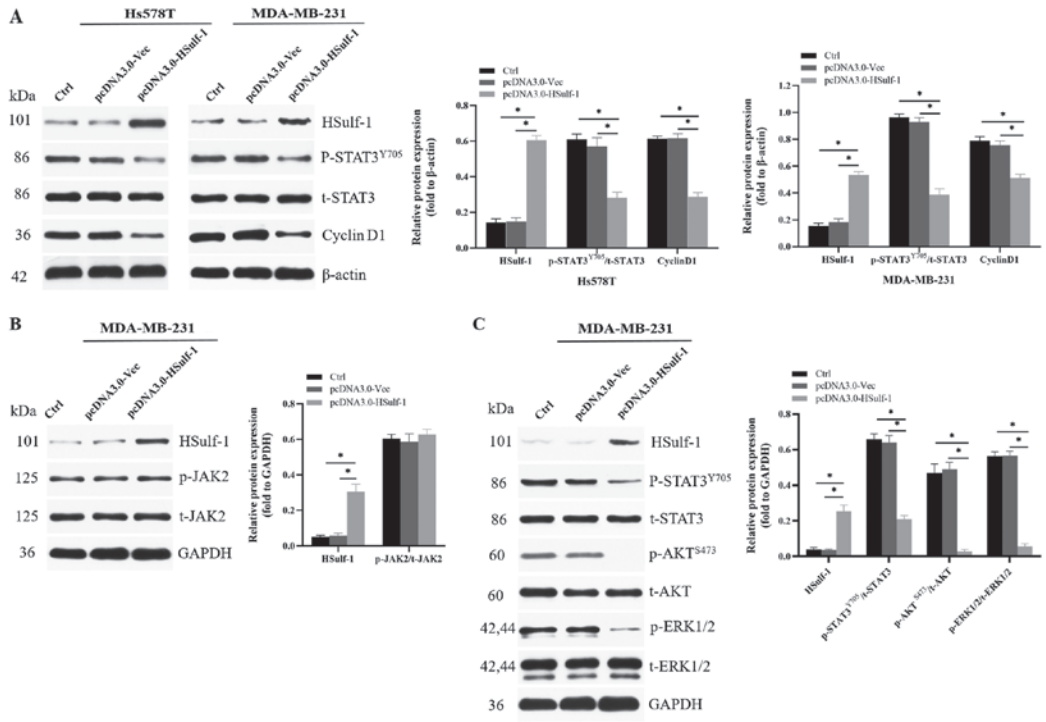

Figure 4. HSulf-1 inhibits cell cycle progression by suppressing the expression of cyclin D1 via non-canonical AKT/STAT3 and ERK1/2/STAT3 signaling. (A) Western blotting was performed to measure the levels of HSulf-1 and cyclin D1 expression in addition to STAT3 phosphorylation in Hs578T and MDA-MB-231 cells following transient transfection with the control vector or HSulf-1 overexpression plasmids. β-Actin was used as an internal control. (B) Western blotting was performed to measure HSulf-1 expression and JAK2 phosphorylation in MDA-MB-231 cells following transient transfection with the control vector or HSulf-1 overexpression plasmids. GAPDH was used as an internal control. (C) Western blotting was performed to measure the expression of HSulf-1 and the degree of phosphorylated ERK1/2, AKT and STAT3 phosphorylation in MDA-MB-231 cells following transient transfection with the control vector or HSulf-1 overexpression plasmids. GAPDH was used as an internal control. The results were derived from three independent experiments. Data are presented as the mean ± SD. *P<0.05. HSulf-1, human sulfatase-1; JAK, janus kinase; vec, vector; ctrl, untransfected control.

leading to significantly lower levels of total RB expression and RB phosphorylation compared with cells transfected with the control vector (Fig. 5A). Finally, the possibility that the aforementioned synergistic effects may be due to a reduction in cyclin D1 expression caused by HSulf-1 overexpression was next considered. Therefore, a rescue experiment was performed on MDA-MB-231 cells, where the overexpression of cyclin D1 abolished the synergistic effects of HSulf-1 and palbociclib treatment on cell proliferation (Fig. 5C and D). Consequently, it was concluded that the mechanism by which HSulf-1 cooperated with palbociclib to exert antiproliferative effects was due to the reversal of palbociclib-induced cyclin D1 accumulation.

Discussion

TNBC is the most heterogeneous sub-type of breast cancer, where gene expression profiling identified six distinct molecular subgroups: Luminal androgen receptor (LAR), mesenchymal stem-like, mesenchymal, two basal-likes and immunomodulatory (21,65). Due to this heterogeneity, patients with TNBC frequently undergo a variety of clinical courses, where a and diverse set of therapeutic responses can occur (21). Therefore, specific therapeutic strategies should be identified based on these molecular sub-types and clinicopathological features. A number of preclinical studies have reported that the RB-positive LAR subgroup of TNBC is sensitive to CDK4/6 inhibitors (43,47,66). However, the anti-metastatic effect of palbociclib on TNBC remains controversial. Lamb *et al* (48) revealed that treatment with palbociclib increased migration and mammosphere formation and had the potential to increase the migratory capacity of TNBC cells, which could in turn increase metastasis and cancer recurrence. Conversely, other studies have previously demonstrated that palbociclib reduced the migration and invasion of TNBC cells in addition to suppressing metastasis in a xenograft metastasis model derived from TNBC cells (49-51). In the present study, RB-positive TNBC cell lines were found to be sensitive to palbociclib, which reduced tumor proliferation both *in vitro* and *in vivo*. Furthermore, palbociclib was found to inhibit TNBC cell migration, invasion and EMT by upregulating E-cadherin expression whilst downregulating that of vimentin and N-cadherin, thus further validating the antitumor effect of palbociclib on RB-positive TNBC.

In recent years, the roles of HSulf-1 in human cancers have attracted attention. HSulf-1 expression was reported to be downregulated in breast cancers, which is considered an early event in the tumorigenesis of breast cancer (37). Additionally, previous studies have demonstrated that HSulf-1 functions as a tumor suppressor in breast cancer; where it can be applied in predicting clinical outcomes (36,38,39). However, these previous studies aforementioned focused primarily on breast cancer without considering the subtype. It is well documented that breast cancer is a highly heterogeneous disease with a complex mechanism of pathogenesis that exhibits a wide range of clinical behaviours and treatment responses. Therefore, it becomes necessary to validate the role of HSulf-1 in TNBC. The present study was specifically

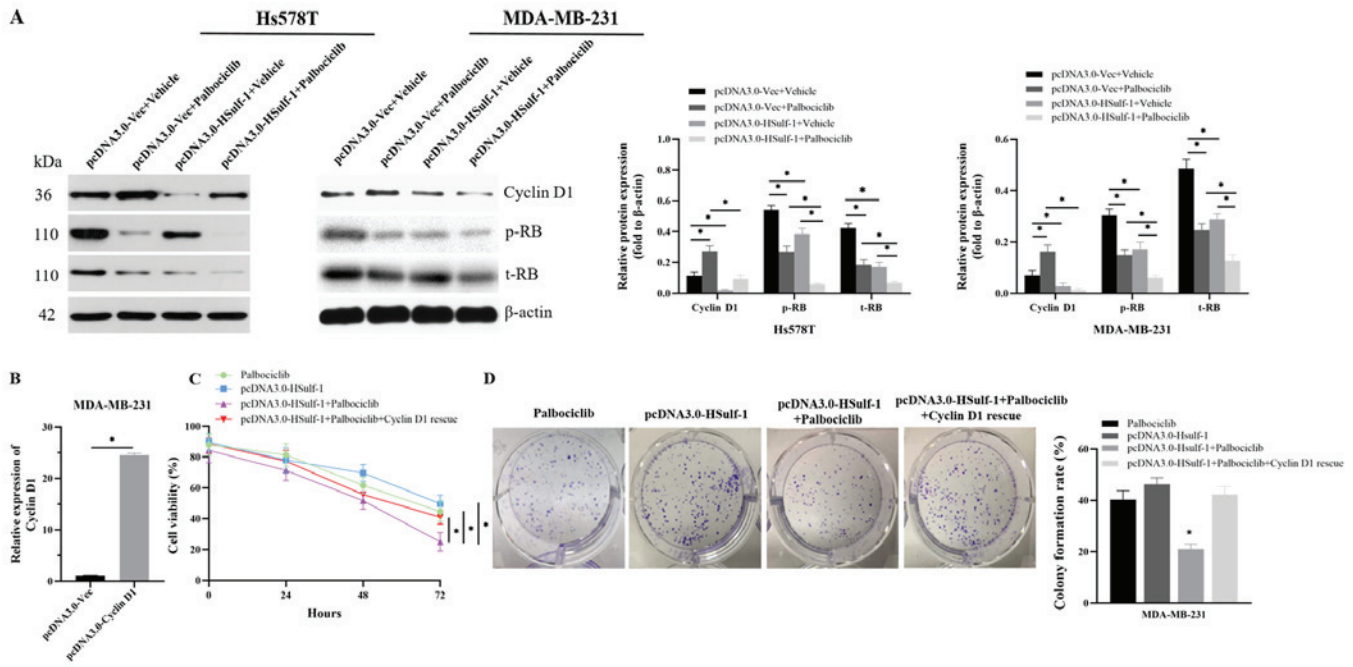

Figure 5. HSulf-1 exhibit synergy with palbociclib to exert antiproliferative effects on breast cancer cells by reducing palbociclib-induced cyclin D1 accumulation. (A) Western blotting was performed to measure the protein levels of cyclin D1, p-RB and total RB in Hs578T and MDA-MB-231 cells following transient transfection with the control vector or HSulf-1 overexpression plasmids and incubation with 500 nM palbociclib or DMSO. β-Actin was used as an internal control. (B) Reverse transcription-quantitative PCR was performed to measure mRNA level of cyclin D1 in MDA-MB-231 cells following transient transfection with the control vector or cyclin D1 overexpression plasmids. GAPDH was used as an internal control. (C) Cell Counting Kit-8 and (D) colony formation assays were performed to evaluate cell viability in MDA-MB-231 cells following incubation with 500 nM palbociclib for 14 days, overexpression of HSulf-1, overexpression of HSulf-1 followed by incubation with 500 nM palbociclib for 14 days or co-transfection of plasmids encoding HSulf-1 and cyclin D1 followed by exposure to palbociclib for 14 days. The results were derived from three independent experiments. Data are presented as the mean ± SD. *P<0.05. HSulf-1, human sulfatase-1; RB, retinoblastoma; p-, phosphorylated; t-, total; vec, vector.

performed on the RB-positive TNBC subtype both *in vitro* and *in vivo*. Accordingly, it was found that HSulf-1 expression was downregulated in TNBC tissues and cells compared with their non-cancerous counterparts. Notably, reduced HSulf-1 expression was highly predictive of poor PFS and OS in patients with TNBC. However, no association was observed between HSulf-1 expression and the other clinicopathological indicators tested, including age, tumor grade, tumor size and lymph nodal status in TNBC tissues. Collectively, these results indicate that HSulf-1 is likely to serve as a reliable prognostic biomarker of patient outcomes for TNBC.

Previous studies have demonstrated that HSulf-1 induces cell cycle arrest and inhibits tumorigenesis and angiogenesis in TNBC cells *in vivo* (36,39). However, the potential effects of HSulf-1 on other physiological processes in TNBC, including apoptosis, migration and invasion, remained unclear. In the present study, it was found that HSulf-1 overexpression inhibited tumor proliferation by inducing G_1/S and G^2/M cell cycle arrest and apoptosis, in accordance with previous reports (19,45,47). In addition, HSulf-1 was also found to suppress migration, invasion and EMT. Collectively, these results demonstrated that HSulf-1 serves as a tumor suppressor in TNBC. Following the discovery that HSulf-1 reduced cyclin D1 expression to induce G_1/S arrest, the hypothesis that HSulf-1 overexpression combined with palbociclib treatment may exhibit synergistic antitumor effects on TNBC cells was investigated. HSulf-1 and palbociclib in combination exerted additive antitumor effects on the induction of G_1/S cell cycle arrest, inhibition of migration, invasion and EMT *in vitro*. Accordingly, this combination may serve as a good alternative therapeutic option for RB-positive TNBC. However, in clinical practice, a suitable vector, including the likes of polyamidoamine dendrimers, transferrin-polyethylene glycol-polyethylenimine and adeno-associated viral vectors, may be required for the effective delivery of the HSulf-1 gene into tumors for patients with TNBC in the future (67-71), which require further clinical validation.

Several studies have previously demonstrated that HBGFs, such as HGF binding to its corresponding receptors c-Met and HSPGs, form a ternary complex to activate downstream tyrosine kinases, resulting in the phosphorylation of substrate proteins, including PI3K-AKT and Ras-MAPK. Desulfation of HSPGs by HSulf-1 prevents the formation of these ternary complexes, followed by the inactivation of downstream signaling pathways (33,34,38,72,73). Therefore, in the context of HBGF signaling, HSPG serves as a coreceptor to facilitate the interaction between the HBGFs and their cognate transducing receptors, activating the phosphorylation cascade. HSulf-1 inhibits the sulfation of cell-surface HSPGs and abrogates growth factor signaling. Mechanisms underlying the regulation of cyclin D1 by HSulf-1 have been proposed. Liu *et al* (56) previously documented that HSulf-1 downregulates cyclin D1 expression by suppressing STAT3 signaling in hepatocellular carcinoma. Notably, the *CCND1* gene was demonstrated to be a target of STAT3, as STAT3-binding sites were identified in the *CCND1* promoter (74). In the present study, HSulf-1 was identified to regulate cyclin D1 expression via non-canonical

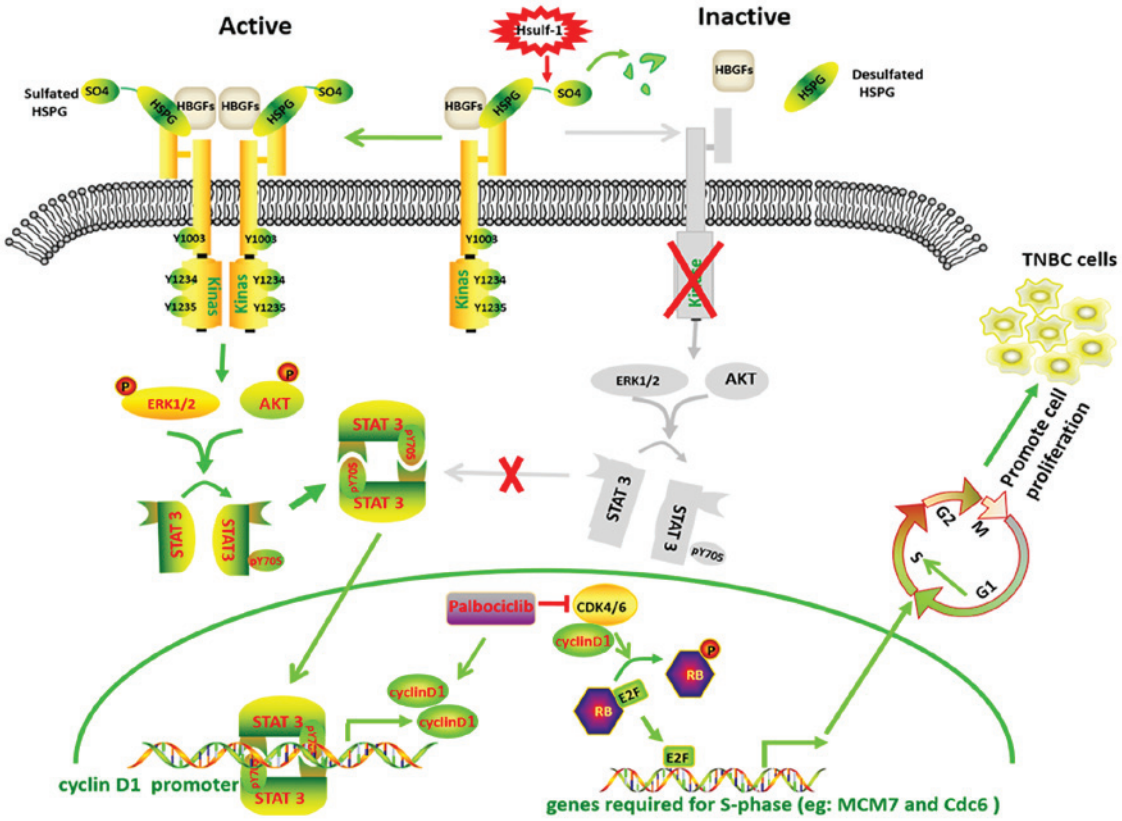

Figure 6. Schematic diagram depicting the possible mechanism of HSulf-1-mediated inactivation of STAT3 via the PI3K/AKT and Ras/ERK1 pathways and crosstalk with CDK-RB-E2F signaling in TNBC cells. The initiation of HBGF signaling requires the binding of extracellular HBGF (FGF, EGF, HGF) and its cognate tyrosine kinase receptor to HSPGs to form a ternary ligand-HSPG-receptor complex at the cell surface. Ligand binding induces receptor dimerization and subsequent phosphorylation of the receptor tyrosine kinase, leading to a downstream phosphorylation cascade including the PI3K/AKT/STAT3 and Ras/ERK1/2/STAT3 pathways. Phosphorylated STAT3 forms a dimer and translocates into the nucleus, promoting cyclin D1 expression. Desulfation of HSPGs by HSulf-1 prevents formation of the ternary complex, leading to a reduction in HBGF signaling and cyclin D1 expression. Hsulf-1, human sulfatase 1; CDK, cyclin-dependent kinase; RB, retinoblastoma; YNBC, triple-negative breast cancer; HBGF, heparin-binding growth factors; HSPG, heparan sulfate proteoglycans; MCM7, minichromosome maintenance complex component 7; cdc6, cell division cycle 6; EGF, epidermal growth factor; FGF, fibroblast growth factor; HGF, hepatocyte growth factor.

AKT/STAT3 and ERK1/2/STAT3 signaling instead of the canonical JAK2/STAT3 pathway. In addition, overexpression of HSulf-1 prevented the apparent increase in cyclin D1 levels caused by palbociclib treatment. Therefore, data from the present study hinted at a potential crosstalk between the HSulf-1/ERK1/2/AKT/STAT3 and CDK-RB-E2F pathways to control cell cycle progression (Fig. 6).

A number of preclinical studies have reported that ER-positive breast cancer cells adapt rapidly to CDK4/6 inhibition to evade cytostasis, in part via non-canonical cyclin D1-CDK2-mediated S phase entry (75). This adaptation was found to be prevented by combining CDK4/6 inhibitors with PI3K/mTOR inhibitors, which reduced the levels of cyclin D1 and other G_1-S phase cyclins (75,76). In the present study, it was also found that the levels of cyclin D1 were increased following palbociclib treatment, consistent with previously reported results (64). This may be due to an adaptive response to damaging stimuli or CDK4/6 inhibitors have a similar negative feedback effect of preventing CDK4/6 to form a complex with cyclin D1, which may increase cyclin D1 expression and further activate the crosstalk between the cyclin D1-CDK2 signaling pathway, which require further study (77). It was previously revealed that STAT3 phosphorylation was significantly increased in palbociclib-resistant ER-positive breast cancer cells, where ER-positive metastatic breast cancer patients acquired resistance after treatment with Palbociclib (78). Furthermore, palbociclib-resistant cells appear to be more sensitive to the STAT3 inhibitor TTI-010, which directly targets the tyrosine-phosphorylated peptide-binding pocket within the STAT3 SH2 domain (78). Based on these observations, HSulf-1 may have the potential to prevent the early adaptation and prolong the durability of palbociclib efficacy in TNBC patients.

Although the present study demonstrated that HSulf-1 overexpression in conjunction with palbociclib has a synergistic antitumor effect in RB-positive TNBC cells. Only the synergistic anti-proliferative mechanism by which HSulf-1 reduced palbociclib-induced cyclin D1 accumulation was clarified. Additionally, although it was demonstrated that HSulf-1 inhibited cyclin D1 expression through the ERK1/2/STAT3 and AKT/STAT3 pathways, it remains unclear whether HSulf-1 could suppresses cyclin D1 expression through other pathways. For the wound healing experiments, it was found that the majority of cells died after 24 h incubation in medium without FBS following scratching a wound introduction. Therefore, medium containing 2% FBS was used, where little or no cell proliferation or cell death were observed. Accordingly, further studies are required to explore these possibilities.

In conclusion, the present study demonstrated that HSulf-1 expression is downregulated in TNBC tissues and cells, which serves an anti-oncogenic role by inducing cell cycle arrest and apoptosis in addition to preventing proliferation, EMT, migration and invasion in TNBC. In addition, it was found that downregulation of HSulf-1 was associated with poor clinical outcomes in patients with TNBC. HSulf-1 inhibited cyclin D1 expression via the non-canonical AKT/STAT3 and ERK1/2/STAT3 signaling pathways in TNBC. In particular, the combination of HSulf-1 overexpression and treatment with the CDK4/6 inhibitor palbociclib exerted additive, synergistic antitumor effects on RB-positive TNBC, which may serve as an effective alternative therapeutic option for patients with RB-positive TNBC.

Acknowledgements

Not applicable.

Funding

This work was supported by the National Natural Science Foundation of China (grant no. 81904231 to FFP) and the Health and Family Planning Commission of Wuhan Municipality (grant no. WX17Q38 to FXC).

Availability of data and materials

The datasets generated during the current study are available from the corresponding author on reasonable request.

Authors' contributions

FP and FC conceived the study and participated in its design and coordination. YY and ZZ performed the experiments and contributed to data collection. FP and FC analyzed the data and drafted the manuscript. ZZ and QL assisted in designing experiments and provided technical expertise in conducting experiments and reviewed the manuscript. All authors read and approved the final version of the manuscript.

Ethics approval and consent to participate

The use of patient tissue samples was approved by the Ethics Committee of the General Hospital of The Yangtze River Shipping, Wuhan Polytechnic University (approval no. 2017IEC0003; Wuhan, China). Informed consent was obtained from all patients. Animal experiments were performed with the approval of the Animal Care and Use Committee of the General Hospital of The Yangtze River Shipping, Wuhan Polytechnic University (approval no. 2017IEC0003; Wuhan, China).

Patient consent for publication

Not applicable.

Competing interests

The authors declare that they have no competing interests.

References

1. Perou CM, Sørlie T, Eisen MB, Van De Rijn M, Jeffrey SS, Rees CA, Pollack JR, Ross DT, Johnsen H, Akslen LA, *et al*: Molecular portraits of human breast tumours. Nature 406: 747-752, 2000.
2. Cancer Genome Atlas Network: Comprehensive molecular portraits of human breast tumours. Nature 490: 61-70, 2012.
3. Rakha EA, El-Rehim DA, Paish C, Green AR, Lee AH, Robertson JF, Blamey RW, Macmillan D and Ellis IO: Basal phenotype identifies a poor prognostic subgroup of breast cancer of clinical importance. Eur J Cancer 42: 3149-3156, 2006.
4. Haffty BG, Yang Q, Reiss M, Kearney T, Higgins SA, Weidhaas J, Harris L, Hait W and Toppmeyer D: Locoregional relapse and distant metastasis in conservatively managed triple negative early-stage breast cancer. J Clin Oncol 24: 5652-5657, 2006.
5. Dent R, Trudeau M, Pritchard KI, Hanna WM, Kahn HK, Sawka CA, Lickley LA, Rawlinson E, Sun P and Narod SA: Triple-negative breast cancer: Clinical features and patterns of recurrence. Clin Cancer Res 13: 4429-4434, 2007.
6. Liedtke C, Mazouni C, Hess KR, André F, Tordai A, Mejia JA, Symmans WF, Gonzalez-Angulo AM, Hennessy B, Green M, *et al*: Response to neoadjuvant therapy and long-term survival in patients with triple-negative breast cancer. J Clin Oncol 26: 1275-1281, 2008.
7. Carey LA, Dees EC, Sawyer L, Gatti L, Moore DT, Collichio F, Ollila DW, Sartor CI, Graham ML and Perou CM: The triple negative paradox: Primary tumor chemosensitivity of breast cancer subtypes. Clin Cancer Res 13: 2329-2334, 2007.
8. Robson M, Im SA, Senkus E, Xu B, Domchek SM, Masuda N, Delaloge S, Li W, Tung N, Armstrong A, *et al*: Olaparib for metastatic breast cancer in patients with a germline BRCA mutation. N Engl J Med 377: 523-533, 2017.
9. Winter C, Nilsson MP, Olsson E, George AM, Chen Y, Kvist A, Törngren T, Vallon-Christersson J, Hegardt C, Häkkinen J, *et al*: Targeted sequencing of BRCA1 and BRCA2 across a large unselected breast cancer cohort suggests that one-third of mutations are somatic. Ann Oncol 27: 1532-1538, 2016.
10. Atchley DP, Albarracin CT, Lopez A, Valero V, Amos CI, Gonzalez-Angulo AM, Hortobagyi GN and Arun BK: Clinical and pathologic characteristics of patients with BRCA-positive and BRCA-negative breast cancer. J Clin Oncol 26: 4282-4288, 2008.
11. Hanahan D and Weinberg RA: The hallmarks of cancer. Cell 100: 57-70, 2000.
12. O'Leary B, Finn RS and Turner NC: Treating cancer with selective CDK4/6 inhibitors. Nat Rev Clin Oncol 13: 417-430, 2016.
13. Finn RS, Crown JP, Lang I, Boer K, Bondarenko IM, Kulyk SO, Ettl J, Patel R, Pinter T, Schmidt M, *et al*: The cyclin-dependent kinase 4/6 inhibitor palbociclib in combination with letrozole versus letrozole alone as first-line treatment of oestrogen receptor-positive, HER2-negative, advanced breast cancer (PALOMA-1/TRIO-18): A randomised phase 2 study. Lancet Oncol 16: 25-35, 2015.
14. Turner NC, Ro J, André F, Loi S, Verma S, Iwata H, Harbeck N, Loibl S, Huang Bartlett C, Zhang K, *et al*: Palbociclib in hormone-receptor-positive advanced breast cancer. N Engl J Med 373: 209-219, 2015.
15. Finn RS, Martin M, Rugo HS, Jones S, Im SA, Gelmon K, Harbeck N, Lipatov ON, Walshe JM, Moulder S, *et al*: Palbociclib and letrozole in advanced breast cancer. N Engl J Med 375: 1925-1936, 2016.
16. Hortobagyi GN, Stemmer SM, Burris HA, Yap YS, Sonke GS, Paluch-Shimon S, Campone M, Blackwell KL, André F, Winer EP, *et al*: Ribociclib as first-line therapy for HR-positive, advanced breast cancer. N Engl J Med 375: 1738-1748, 2016.
17. Tripathy D, Im SA, Colleoni M, Franke F, Bardia A, Harbeck N, Hurvitz SA, Chow L, Sohn J, Lee KS, *et al*: Ribociclib plus endocrine therapy for premenopausal women with hormone-receptor-positive, advanced breast cancer (MONALEESA-7): A randomised phase 3 trial. Lancet Oncol 19: 904-915, 2018.
18. Sledge GW Jr, Toi M, Neven P, Sohn J, Inoue K, Pivot X, Burdaeva O, Okera M, Masuda N, Kaufman PA, *et al*: MONARCH 2: Abemaciclib in combination with fulvestrant in women with HR+/HER2-advanced breast cancer who had progressed while receiving endocrine therapy. J Clin Oncol 35: 2875-2884, 2017.
19. Finn RS, Dering J, Conklin D, Kalous O, Cohen DJ, Desai AJ, Ginther C, Atefi M, Chen I, Fowst C, *et al*: PD 0332991, a selective cyclin D kinase 4/6 inhibitor, preferentially inhibits proliferation of luminal estrogen receptor-positive human breast cancer cell lines in vitro. Breast Cancer Res 11: R77, 2009.

20. DeMichele A, Clark AS, Tan KS, Heitjan DF, Gramlich K, Gallagher M, Lal P, Feldman M, Zhang P, Colameco C, *et al*: CDK 4/6 inhibitor palbociclib (PD0332991) in Rb+ advanced breast cancer: Phase II activity, safety, and predictive biomarker assessment. Clin Cancer Res 21: 995-1001, 2015.
21. Lehmann BD, Bauer JA, Chen X, Sanders ME, Chakravarthy AB, Shyr Y and Pietenpol JA: Identification of human triple-negative breast cancer subtypes and preclinical models for selection of targeted therapies. J Clin Invest 121: 2750-2767, 2011.
22. Witkiewicz AK and Knudsen ES: Retinoblastoma tumor suppressor pathway in breast cancer: Prognosis, precision medicine, and therapeutic interventions. Breast Cancer Res 16: 207, 2014.
23. Treré D, Brighenti E, Donati G, Ceccarelli C, Santini D, Taffurelli M, Montanaro L and Derenzini M: High prevalence of retinoblastoma protein loss in triple-negative breast cancers and its association with a good prognosis in patients treated with adjuvant chemotherapy. Ann Oncol 20: 1818-1823, 2009.
24. Witkiewicz AK, Ertel A, McFalls J, Valsecchi ME, Schwartz G and Knudsen ES: RB-pathway disruption is associated with improved response to neoadjuvant chemotherapy in breast cancer. Clin Cancer Res 18: 5110-5122, 2012.
25. Lamanna WC, Frese MA, Balleininger M and Dierks T: Sulf loss influences N-, 2-O-, and 6-O-sulfation of multiple heparan sulfate proteoglycans and modulates fibroblast growth factor signaling. J Biol Chem 283: 27724-27735, 2008.
26. Dhoot GK, Gustafsson MK, Ai X, Sun W, Standiford DM and Emerson CP Jr: Regulation of Wnt signaling and embryo patterning by an extracellular sulfatase. Science 293: 1663-1666, 2001.
27. Takashima Y, Keino-Masu K, Yashiro H, Hara S, Suzuki T, van Kuppevelt TH, Masu M and Nagata M: Heparan sulfate 6-O-endosulfatases, Sulf1 and Sulf2, regulate glomerular integrity by modulating growth factor signaling. Am J Physiol Renal Physiol 310: F395-F408, 2016.
28. Chen Z, Fan JQ, Li J, Li QS, Yan Z, Jia XK, Liu WD, Wei LJ, Zhang FZ, Gao H, *et al*: Promoter hypermethylation correlates with the Hsulf-1 silencing in human breast and gastric cancer. Int J Cancer 124: 739-744, 2009.
29. Staub J, Chien J, Pan Y, Qian X, Narita K, Aletti G, Scheerer M, Roberts LR, Molina J and Shridhar V: Epigenetic silencing of HSulf-1 in ovarian cancer: Implications in chemoresistance. Oncogene 26: 4969-4978, 2007.
30. Lai JP, Sandhu DS, Shire AM and Roberts LR: The tumor suppressor function of human sulfatase 1 (SULF1) in carcinogenesis. J Gastrointest Cancer 39: 149-158, 2008.
31. Marotta LL, Almendro V, Marusyk A, Shipitsin M, Schemme J, Walker SR, Bloushtain-Qimron N, Kim JJ, Choudhury SA, Maruyama R, *et al*: The JAK2/STAT3 signaling pathway is required for growth of CD44(+)CD24(-) stem cell-like breast cancer cells in human tumors. J Clin Invest 121: 2723-2735, 2011.
32. Dai Y, Yang Y, MacLeod V, Yue X, Rapraeger AC, Shriver Z, Venkataraman G, Sasisekharan R and Sanderson RD: HSulf-1 and HSulf-2 are potent inhibitors of myeloma tumor growth in vivo. J Biol Chem 280: 40066-40073, 2005.
33. Lai JP, Chien JR, Moser DR, Staub JK, Aderca I, Montoya DP, Matthews TA, Nagorney DM, Cunningham JM, Smith DI, *et al*: hSulf1 Sulfatase promotes apoptosis of hepatocellular cancer cells by decreasing heparin-binding growth factor signaling. Gastroenterology 126: 231-248, 2004.
34. Lai JP, Chien J, Strome SE, Staub J, Montoya DP, Greene EL, Smith DI, Roberts LR and Shridhar V: HSulf-1 modulates HGF-mediated tumor cell invasion and signaling in head and neck squamous carcinoma. Oncogene 23: 1439-1447, 2004.
35. Roy D, Mondal S, Wang C, He X, Khurana A, Giri S, Hoffmann R, Jung DB, Kim SH, Chini EN, *et al*: Loss of HSulf-1 promotes altered lipid metabolism in ovarian cancer. Cancer Metab 2: 13, 2014.
36. Narita K, Staub J, Chien J, Meyer K, Bauer M, Friedl A, Ramakrishnan S and Shridhar V: HSulf-1 inhibits angiogenesis and tumorigenesis in vivo. Cancer Res 66: 6025-6032, 2006.
37. Lai J, Chien J, Staub J, Avula R, Greene EL, Matthews TA, Smith DI, Kaufmann SH, Roberts LR and Shridhar V: Loss of HSulf-1 up-regulates heparin-binding growth factor signaling in cancer. J Biol Chem 278: 23107-23117, 2003.
38. Khurana A, Liu P, Mellone P, Lorenzon L, Vincenzi B, Datta K, Yang B, Linhardt RJ, Lingle W, Chien J, *et al*: HSulf-1 modulates FGF2- and hypoxia-mediated migration and invasion of breast cancer cells. Cancer Res 71: 2152-2161, 2011.
39. Narita K, Chien J, Mullany SA, Staub J, Qian X, Lingle WL and Shridhar V: Loss of HSulf-1 expression enhances autocrine signaling mediated by amphiregulin in breast cancer. J Biol Chem 282: 14413-14420, 2007.
40. Böcker W: WHO Classification of Breast Tumors and Tumors of the Female Genital Organs: Pathology and Genetics. Verh Dtsch Ges Pathol 86: 116-119, 2002.
41. Amin MB, Edge S, Greene F, Byrd DR, Brookland RK, Washington MK, Gershenwald JE, Compton CC, Hess KR, Sullivan DC, *et al*: AJCC cancer staging manual 8th ed. New York: Springer, 2017.
42. Dean JL, McClendon AK and Knudsen ES: Modification of the DNA damage response by therapeutic CDK4/6 inhibition. J Biol Chem 287: 29075-29087, 2012.
43. Asghar US, Barr AR, Cutts R, Beaney M, Babina I, Sampath D, Giltnane J, Lacap JA, Crocker L, Young A, *et al*: Single-cell dynamics determines response to CDK4/6 inhibition in triple-negative breast cancer. Clin Cancer Res 23: 5561-5572, 2017.
44. Livak KJ and Schmittgen TD: Analysis of relative gene expression data using real-time quantitative PCR and the 2(-Delta Delta C(T)) method. Methods 25: 402-408, 2001.
45. Yamamoto T, Kanaya N, Somlo G and Chen S: Synergistic anti-cancer activity of CDK4/6 inhibitor palbociclib and dual mTOR kinase inhibitor MLN0128 in pRb-expressing ER-negative breast cancer. Breast Cancer Res Treat 174: 615-625, 2019.
46. Foidart P, Yip C, Radermacher J, Blacher S, Lienard M, Montero-Ruiz L, Maquoi E, Montaudon E, Château-Joubert S, Collignon J, *et al*: Expression of MT4-MMP, EGFR, and RB in triple-negative breast cancer strongly sensitizes tumors to erlotinib and palbociclib combination therapy. Clin Cancer Res 25: 1838-1850, 2019.
47. Liu CY, Lau KY, Hsu CC, Chen JL, Lee CH, Huang TT, Chen YT, Huang CT, Lin PH and Tseng LM: Combination of palbociclib with enzalutamide shows in vitro activity in RB proficient and androgen receptor positive triple negative breast cancer cells. PLoS One 12: e0189007, 2017.
48. Lamb R, Lehn S, Rogerson L, Clarke RB and Landberg G: Cell cycle regulators cyclin D1 and CDK4/6 have estrogen receptor-dependent divergent functions in breast cancer migration and stem cell-like activity. Cell cycle 12: 2384-2394, 2013.
49. Zhong Z, Yeow WS, Zou C, Wassell R, Wang C, Pestell RG, Quong JN and Quong AA: Cyclin D1/cyclin-dependent kinase 4 interacts with filamin A and affects the migration and invasion potential of breast cancer cells. Cancer Res 70: 2105-2114, 2010.
50. Liu T, Yu J, Deng M, Yin Y, Zhang H, Luo K, Qin B, Li Y, Wu C, Ren T, *et al*: CDK4/6-dependent activation of DUB3 regulates cancer metastasis through SNAIL1. Nat Commun 8: 13923, 2017.
51. Qin G, Xu F, Qin T, Zheng Q, Shi D, Xia W, Tian Y, Tang Y, Wang J, Xiao X, *et al*: Palbociclib inhibits epithelial-mesenchymal transition and metastasis in breast cancer via c-Jun/COX-2 signaling pathway. Oncotarget 6: 41794-41808, 2015.
52. Tsai JH and Yang J: Epithelial-mesenchymal plasticity in carcinoma metastasis. Genes Dev 27: 2192-2206, 2013.
53. Kang Y and Massague J: Epithelial-mesenchymal transitions: Twist in development and metastasis. Cell 118: 277-279, 2004.
54. Thiery JP, Acloque H, Huang RY and Nieto MA: Epithelial-mesenchymal transitions in development and disease. Cell 139: 871-890, 2009.
55. Ye X and Weinberg RA: Epithelial-mesenchymal plasticity: A central regulator of cancer progression. Trends Cell Biol 25: 675-686, 2015.
56. Liu L, Ding F, Chen J, Wang B and Liu Z: hSulf-1 inhibits cell proliferation and migration and promotes apoptosis by suppressing stat3 signaling in hepatocellular carcinoma. Oncol Lett 7: 963-969, 2014.
57. Banerjee K and Resat H: Constitutive activation of STAT3 in breast cancer cells: A review. Int J Cancer 138: 2570-2578, 2016.
58. Bao L, Yan Y, Xu C, Ji W, Shen S, Xu G, Zeng Y, Sun B, Qian H, Chen L, *et al*: MicroRNA-21 suppresses PTEN and hSulf-1 expression and promotes hepatocellular carcinoma progression through AKT/ERK pathways. Cancer Lett 337: 226-236, 2013.
59. Liu H, Fu X, Ji W, Liu K, Bao L, Yan Y, Wu M, Yang J and Su C: Human sulfatase-1 inhibits the migration and proliferation of SMMC-7721 hepatocellular carcinoma cells by downregulating the growth factor signaling. Hepatol Res 43: 516-525, 2013.

60. Xu G, Ji W, Su Y, Xu Y, Yan Y, Shen S, Li X, Sun B, Qian H, Chen L, *et al*: Sulfatase 1 (hSulf-1) reverses basic fibroblast growth factor-stimulated signaling and inhibits growth of hepatocellular carcinoma in animal model. Oncotarget 5: 5029-5039, 2014.
61. Zhang H, Newman DR and Sannes PL: HSULF-1 inhibits ERK and AKT signaling and decreases cell viability in vitro in human lung epithelial cells. Respir Res 13: 69, 2012.
62. Corsetti G, Yuan Z, Romano C, Chen-Scarabelli C, Fanzani A, Pasini E, Dioguardi FS, Onorati F, Linardi D, Knight R, *et al*: Urocortin induces phosphorylation of distinct residues of signal transducer and activator of transcription 3 (STAT3) via different signaling pathways. Med Sci Monit Basic Res 25: 139-152, 2019.
63. Malanga D, De Marco C, Guerriero I, Colelli F, Rinaldo N, Scrima M, Mirante T, De Vitis C, Zoppoli P, Ceccarelli M, *et al*: The Akt1/IL-6/STAT3 pathway regulates growth of lung tumor initiating cells. Oncotarget 6: 42667-42686, 2015.
64. Long F, He Y, Fu H, Li Y, Bao X, Wang Q, Wang Y, Xie C and Lou L: Preclinical characterization of SHR6390, a novel CDK 4/6 inhibitor, in vitro and in human tumor xenograft models. Cancer Sci 110: 1420-1430, 2019.
65. Burstein MD, Tsimelzon A, Poage GM, Covington KR, Contreras A, Fuqua SA, Savage MI, Osborne CK, Hilsenbeck SG, Chang JC, *et al*: Comprehensive genomic analysis identifies novel subtypes and targets of triple-negative breast cancer. Clin Cancer Res 21: 1688-1698, 2015.
66. Asghar U, Herrera-Abreu MT, Cutts R, Babina I, Pearson A and Turner NC: Identification of subtypes of triple negative breast cancer (TNBC) that are sensitive to CDK4/6 inhibition. J Clin Oncol 33: 11098, 2015.
67. Rein DT, Breidenbach M and Curiel DT: Current developments in adenovirus-based cancer gene therapy. Future Oncol 2: 137-143, 2006.
68. Maruyama TH, Harada Y, Matsumura T, Satoh E, Cui F, Iwai M, Kita M, Hibi S, Imanishi J, Sawada T and Mazda O: Effective suicide gene therapy in vivo by EBV-based plasmid vector coupled with polyamidoamine dendrimer. Gene Ther 7: 53-60, 2000.
69. Kursa M, Walker GF, Roessler V, Ogris M, Roedl W, Kircheis R and Wagner E: Novel shielded transferrin-polyethylene glycol-polyethylenimine/DNA complexes for systemic tumor-targeted gene transfer. Bioconjug Chem 14: 222-231, 2003.
70. Griffin JM, Fackelmeier B, Clemett CA, Fong DM, Mouravlev A, Young D and O'Carroll SJ: Astrocyte-selective AAV-ADAMTS4 gene therapy combined with hindlimb rehabilitation promotes functional recovery after spinal cord injury. Exp Neurol 327: 113232, 2020.
71. Salameh JW, Zhou L, Ward SM, Chalaarca CF, Emrick T and Figueiredo ML: Polymer-mediated gene therapy: Recent advances and merging of delivery techniques. Wiley Interdiscip Rev Nanomed Nanobiotechnol 12: e1598, 2020.
72. Selva EM and Perrimon N: Role of heparan sulfate proteoglycans in cell signaling and cancer. Adv Cancer Res 83: 67-80, 2001.
73. Rubin JS, Day RM, Breckenridge D, Atabey N, Taylor WG, Stahl SJ, Wingfield PT, Kaufman JD, Schwall R and Bottaro DP: Dissociation of heparan sulfate and receptor binding domains of hepatocyte growth factor reveals that heparan sulfate-c-met interaction facilitates signaling. J Biol Chem 276: 32977-32983, 2001.
74. Bromberg JF, Wrzeszczynska MH, Devgan G, Zhao Y, Pestell RG, Albanese C and Darnell JE Jr: Stat3 as an oncogene. Cell 98: 295-303, 1999.
75. Herrera-Abreu MT, Palafox M, Asghar U, Rivas MA, Cutts RJ, Garcia-Murillas I, Pearson A, Guzman M, Rodriguez O, Grueso J, *et al*: Early adaptation and acquired resistance to CDK4/6 inhibition in estrogen receptor-positive breast cancer. Cancer Res 76: 2301-2313, 2016.
76. Michaloglou C, Crafter C, Siersbaek R, Delpuech O, Curwen JO, Carnevalli LS, Staniszewska AD, Polanska UM, Cheraghchi-Bashi A, Lawson M, *et al*: Combined inhibition of mTOR and CDK4/6 is required for optimal blockade of E2F function and long-term growth inhibition in estrogen receptor-positive breast cancer. Mol Cancer Ther 17: 908-920, 2018.
77. Javle MM, Shroff RT, Xiong H, Varadhachary GA, Fogelman D, Reddy SA, Davis D, Zhang Y, Wolff RA and Abbruzzese JL: Inhibition of the mammalian target of rapamycin (mTOR) in advanced pancreatic cancer: Results of two phase II studies. BMC Cancer 10: 368, 2010.
78. Kettner NM, Vijayaraghavan S, Durak MG, Bui T, Kohansal M, Ha MJ, Liu B, Rao X, Wang J, Yi M, *et al*: Combined inhibition of STAT3 and DNA repair in palbociclib-resistant ER-positive breast cancer. Clin Cancer Res 25: 3996-4013, 2019.